European Journal of Gynaecological Oncology

Eur. J. Gynaecol. Oncol. **2022**; 43(1): 48–55
http://doi.org/10.31083/j.ejgo4301013

Original Research

Huwe1 inactivation promotes ovarian cancer metastasis by extracellular matrix deregulation

Fujuan Zhang[1,†], Jing Guo[1,†], Shuaishuai Yu[1], Xudong Zhao[1,2], Yongxin Ma[1,*], Dong Yang[1,2,*]

[1]Laboratory of Animal Tumor Models, Frontiers Science Center for Disease-related Molecular Network, State Key Laboratory of Biotherapy and Cancer Center, West China Hospital, Sichuan University, 610041 Chengdu, Sichuan, China
[2]Kunming Institute of Zoology, Chinese Academy of Sciences, 650223 Kunming, Yunnan, China
*Correspondence: yangdong@wchscu.cn (Dong Yang); mayongxin@gmail.com (Yongxin Ma)
†These authors contributed equally.
Academic Editor: Enrique Hernandez
Submitted: 12 October 2021 Revised: 25 November 2021 Accepted: 29 November 2021 Published: 15 February 2022

Abstract

Objective: *Huwe1* is critical for promoting the progression of a range of malignancies including ovarian cancer. Still, its role in ovarian cancer metastasis has not been reported. The goal of our study was to evaluate a correlation between *Huwe1* and ovarian cancer metastasis. **Methods**: The mouse ovary surface epithelium (MOSE) cells isolated from *Huwe1*$^{L/L}$ mice were identified by flow cytometry assay. Cell migration and invasion were analyzed by transwell system. The molecular mechanism of *Huwe1* in ovarian cancer migration and invasion was explored by analyzing the difference of RNAseq data between MOSE-*Huwe1*$^{L/L}$-CreER and MOSE-*Huwe1*$^{L/L}$-Cre cells. **Results**: *Huwe1* deletion significantly promoted tumor migration and invasion in ovarian cancer cells. Moreover, tumor cells were more frequently detected in the blood when the mice bearing allografts were treated with tamoxifen. Transcriptome analysis indicated that this phenotype may be due to the alteration in cell adhesion caused by the *Huwe1* knockout. **Conclusion**: *Huwe1* inactivation promoted ovarian cancer metastasis by the extracellular matrix (ECM) deregulation.

Keywords: *Huwe1*; Invasion; Ovarian cancer; MOSE cells; Extracellular matrix

1. Introduction

Roles of the *Huwe1*, an E3 ligase, in DNA damage accumulation and tumor initiation, progression, and metastasis are critical. It degrades numerous tumor suppression and promotion substrates, such as Myc, BRCA1, TIAM1, H2AX, p53 and CDC6 [1]. Due to the complexity of its substrate, its roles in cancer remain controversial. *Huwe1* served oncogenic roles in breast and prostate cancer, while it served anti-oncogenic roles in certain lung cancers and colorectal cancer [2]. Additionally, only a few studies have demonstrated the effect of *Huwe1* on tumor metastasis, and the results were contradictory. In human lung cancers, *Huwe1* stimulates cell metastasis by modulating the stability of TIAM1 [3]. In contrast, loss of *Huwe1* promoted thyroid cancer cells migration and invasion in allografts [4]. The conflicting data indicated that the role of *Huwe1* in tumor metastasis was likely to be cell type-dependent in response to different genetic change.

Ovarian cancer is common malignant tumors of the female genital organs. Because the ovary is located deep inside the pelvis, ovarian cancer is generally asymptomatic in prophase, and typically diagnosed in the terminal stage. Seventy percent of ovarian cancers would have spread to the greater omentum of the uterine adnexa, and various organs of the pelvis at the time of diagnosis [5]. Therefore, identification of key genes involved in ovarian metastasis may be beneficial for ovarian cancer treatment [6].

It was reported that high *Huwe1* expression in patients with ovarian cancer was associated with worse prognosis [7,8]. Our previous study confirmed *Huwe1* sustained tumor growth via the histone H1.3-H19 cascade [9]. However, the function of *Huwe1* in ovarian cancer metastasis was still unclear. Here, MOSE cells were isolated and infected according to previous methods [9]. Subsequently, the potential roles of *Huwe1* in ovarian cancer tumor metastasis were investigated, and the results showed that cell migration and invasion were promoted by *Huwe1* inactivation *in vitro*. It was also shown that tumor cells were more frequently detected in the blood of the mice bearing allografts when *Huwe1* was deleted by tamoxifen. Further studies suggested that the phenotype may be caused by deregulation of the extracellular matrix (ECM) induced by *Huwe1* inactivation.

2. Materials and methods

2.1 Cell culture

MOSE cells were isolated from *Huwe1*$^{L/L}$ mice according to previously described methods [10]. OVCAR3, SKOV-3 and HEK293T cells were cultured in DMEM supplemented with 10% FBS at 37 °C, 5% CO_2, and identified by short tandem repeat (STR) profiling.

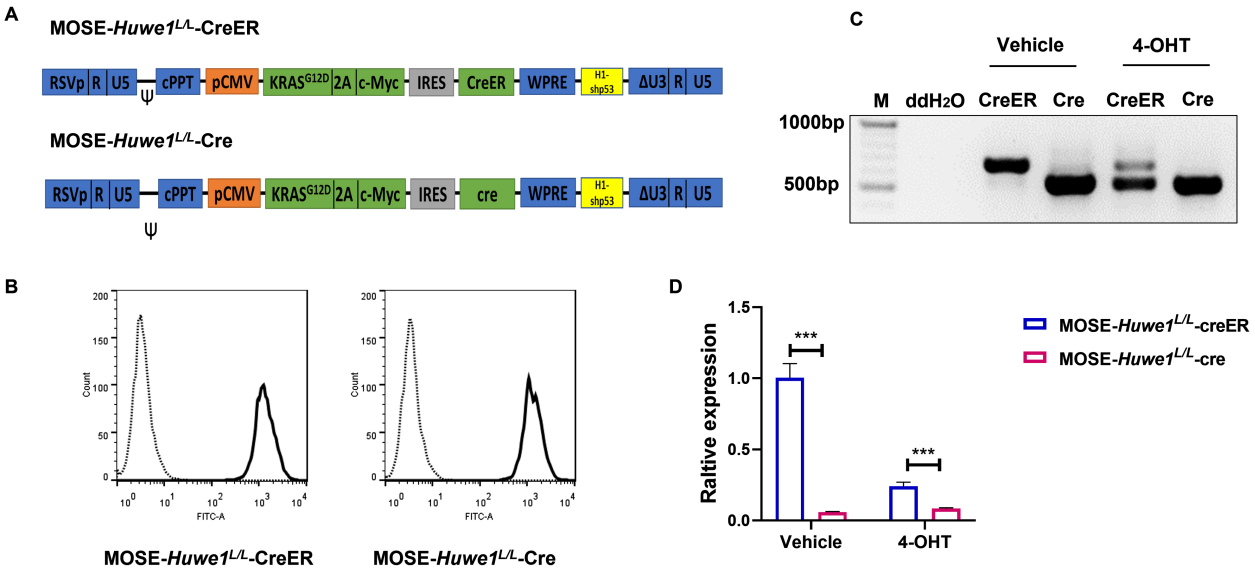

Fig. 1. Knockout of the *Huwe1* gene in MOSE cells. (A) The lentiviral vectors structure for inducing MOSE cells malignant transformation *in vitro*. (B) Identification of CK8-positive ovarian epithelial cells by flow cytometry. (C) Genotyping PCR shows that *Huwe1* was deleted by Cre or treatment with 4-OHT in CreER expressing cells. (D) qRT-PCR analysis of *Huwe1* mRNA expression. The results are indicated as the mean ± SD. *, $p < 0.05$, **, $p < 0.01$, ***, $p \leq 0.001$.

2.2 Plasmid construction and lentiviral preparation

The lentiviral vectors pTomo-pCMV-KRAS^{G12D}-2A-MYC-IRES-Cre-*shp53* and pTomo-pCMV-KRAS^{G12D}-2A-MYC-IRES-CreER-*shp53* were previously constructed by laboratory personnel [11]. For lentivirus production, the core vectors and the helper plasmids pCMVΔ8.9, pMD2.G were co-transfected into HEK293T cells at the ratio of 10:5:2 as described by Dong Yang *et al.* [9].

2.3 Quantitative Real-time PCR (qRT-PCR)

Total RNA was isolated using TRIzol reagent (Sigma-Aldrich, USA). DNA contaminants were removed by the TURBO DNA-free TM Kit (Invitrogen, USA). Subsequently, 2 μg of processed RNA was reverse transcribed by the Revert Aid First Strand cDNA Synthesis kit (Thermo Scientific, USA). Quantitative PCR was carried out in triplicate using the SYBR Green method (Life Technologies, USA). All operations were performed according to the manufacturer's protocols. All the primers used in this study are listed in **Supplementary Table 1.**

2.4 RNAseq analysis

The top-scored reads prioritized by FastQC v0.11.2 (available online at https://www.bioinformatics.babraham.ac.uk/projects/fastqc/) achieved higher alignment accuracies. After sequencing, raw data were filtered to remove undesired reads. Clean reads were mapped to the mouse genome (version GRCm38.p4, which contained 21,936 protein-coding and 3495 lincRNA genes) using Tophat-2.1.0. Genes were defined distinctly up- or down-regulated when a false discovery rate (FDR)-adjusted p value ≤ 0.05 and an absolute value of fold change ≥ 3 using Cuffdiff [12]. The raw RNAseq data has been deposited into the SRA database on the NCBI website (Accession No. SRP081212).

2.5 Wound-healing assay

Cells were cultured to approximately 80% confluence in 6-well culture dishes. After mitomycin C (sigma, USA, 5 μg/mL) treatment was carried out, monolayer wounds were made by scratching with 200 μL pipette tips. Next, the cells were permitted to migrate into the wounded area for 8 h, and the scoring of cells in each well was recorded using a microscope. Cells migration was determined through measuring the width of the scratched area using ImageJ^{TM} software (version 1.8.0, NIH, Bethesda, MD, USA).

2.6 Transwell invasion assay

To inhibit cell proliferation, the cells were processed using mitomycin C (5 μg/mL). Then, the cells were suspended in a serum-free medium, followed by inoculation in the upper migration chamber (Corning, NY, USA), precoated with Matrigel (BD Biosciences, San Jose, NJ, USA). The medium containing 10% FBS was added to the bottom migration chamber. After 8 h of directional migration, the upper insert was carefully removed. The cells on the bottom transwell chamber fixed in methanol, then stained with 0.1% crystal violet. After 30 min, the crystal violet was eluted via 10% acetic acid, and the absorbance of crystal violet solution was measured at 570 nm on a microplate reader.

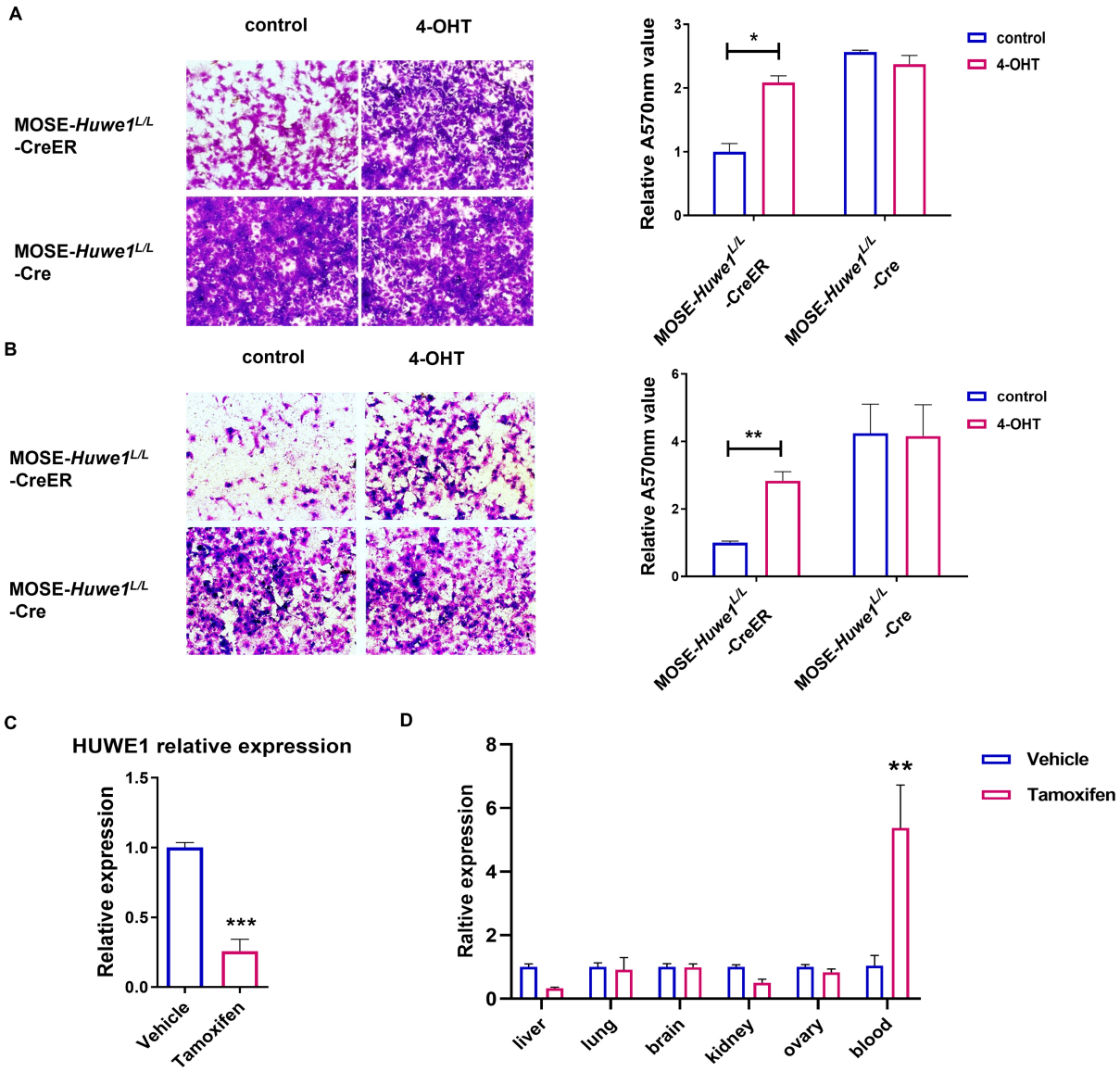

Fig. 2. Loss of *Huwe1* promoted MOSE cells migration and invasion and affected their distribution in mouse models. (A) Analyzing the migration of MOSE-$Huwe1^{L/L}$-CreER cells and MOSE-$Huwe1^{L/L}$-Cre. The left and right images show the crystal violet staining in the transwell chamber migration analysis and the measured absorbance values after elution respectively. Scale bar, 100 μm. (B) Detecting the invasion of MOSE-$Huwe1^{L/L}$-CreER cells and MOSE-$Huwe1^{L/L}$-Cre. The left and right images show the crystal violet staining in the transwell chamber invasion analysis and the measured absorbance values after elution respectively. Scale bar, 100 μm. (C,D) The mice bearing allograft tumors were administered by tamoxifen or vehicle every other day for 18 days, *Huwe1* expression in allograft tumors was detected by qRT-PCR (C). The number of tumor cells in different tissues were detected by quantifying the copy number of exogenous KRAS-2A-MYC in DNA using qRT-PCR (D). The results are indicated as the mean $\pm$ SD. *, $p < 0.05$, **, $p < 0.01$, ***, $p \leq 0.001$.

2.7 Allograft mouse models of ovarian cancer

A total of 2×10^6 MOSE cells expressing $KRAS^{G12D}$-2A-MYC-IRES-CreER-*shp53* elements were injected subcutaneously into six weeks old BALB/c nude mice. After the subcutaneous tumors attained about 5–8 mm in diameter, tamoxifen or vehicle was administered by intraperitoneal injection every other day for 18 days until the end of the experiment. DNA was extracted from major tissues of mice and submitted to quantitative qRT-PCR to detect metastatic cells. The primer was located in the exogenous KRAS-2A-MYC element, and the sequence was listed in **Supplementary Table 1**.

2.8 Statistical analysis

All statistical analyses were carried out using GraphPad Prism 7 (GraphPad Prism, USA). The data are indicated

as mean ± SD. Statistical difference was analyzed using an unpaired Student's *t*-test. Statistical significance was defined as $*p \leq 0.05$, $**p \leq 0.01$, $***p \leq 0.001$.

3. Results

3.1 Huwe1 deletion promoted MOSE cells migration and invasion

To evaluate the roles of *Huwe1* in ovarian cancer metastasis, the MOSE cells were isolated as previously described [9]. The MOSE cell infected by the vectors named MOSE-*Huwe1*$^{L/L}$-Cre or MOSE-*Huwe1*$^{L/L}$-CreER, respectively (Fig. 1A). Hereafter, MOSE cells will be adopted to refer to infected MOSE cells unless otherwise stated. To identify the type of isolated cells, a flow cytometry assay was applied, and the results indicated that almost all the tested cells expressed ovarian epithelial cells marker CK8 (Fig. 1B). To delete the *Huwe1* gene, a Cre or CreER element was subcloned into the lentiviral vectors. *Huwe1* expression was not detectable in cells expressing Cre. When CreER translocated into the nucleus mediated by 4-hydroxytamoxifen (4-OHT), the exons in most MOSE cells were also removed (Fig. 1C–D). To explore the effects of *Huwe1* on cell migration, a wound healing assay was carried out in MOSE cells (**Supplementary Fig. 1**). The results suggested that *Huwe1* deletion significantly promoted the migration of MOSE cells into the central wound area. To further verify the result, a transwell migration assay was also done to test the migration of MOSE cells (Fig. 2A). Consistent with the wound healing assay results, *Huwe1*-null cells migrated into the lower compartment of the migration chamber more frequently than the *Huwe1*-wild cells. These results proved that *Huwe1* significantly repressed the migration ability of MOSE cells *in vitro*. The Boyden chamber was modified with a thin layer of Matrigel to mimic the three-dimensional (3D) cell culture environment, and then the MOSE cells were cultured in the upper chambers to investigate the roles of *Huwe1* in cell invasion potential. 8 hours later, the number of *Huwe1*-null cells reaching the other side of the filter was much higher than that of *Huwe1*-wild cells (Fig. 2B). All the above results proved that *Huwe1* deletion promoted MOSE cells migration and invasion *in vitro*. We subcutaneously injected *Huwe1*$^{L/L}$*-CreER* cells into mice and used tamoxifen to induce *Huwe1* deletion (**Supplementary Fig. 2**). First, we examined *Huwe1* expression in mice when *Huwe1*$^{L/L}$*-CreER* allografts were induced with tamoxifen (Fig. 2C). The results showed that tamoxifen treatment significantly induced *Huwe1* deletion. To observe the distribution of tumor cells in mice, we then investigated the number of tumor cells in each tissue, and only a small difference was observed in the liver and kidney tissues, whereas the number of tumor cells in the blood increased significantly (Fig. 2D).

3.2 Silencing Huwe1 promoted human ovarian cancer cell migration and invasion

To further explore the phenotype of *Huwe1* loss in human ovarian cancer cells, SKOV-3 and OVCAR-3 cells were infected via lentivirus expressing tetracycline-inducible *Huwe1* shRNA (teton-sh*Huwe1*). After the SKOV-3 and OVCAR-3 cells were infected with a teton-sh*Huwe1* lentivirus, they were treated with tetracycline for 5 days. *Huwe1* silencing was demonstrated in DOX-treated cells (Fig. 3A). We performed transwell assays to explore the roles of *Huwe1* in SKOV-3 and OVCAR3 cell migration as well as invasion. *Huwe1* knockdown evidently increased the number of invading cells compared with the untreated group, indicating that *Huwe1* effectively inhibited SKOV-3 cells migration and invasion (Fig. 3B,C). Similarly, *Huwe1* knockdown also significantly increased OVCAR3 migration. However, OVCAR3 cells failed to penetrate the basement membrane for invasion (Fig. 3D). This may be caused by the lower invasive capacity of OVCAR3 cells. The results confirmed that *Huwe1* also had a similar function in human ovarian cancer cell.

3.3 Huwe1 inactivation promoted cancer metastasis by dysregulation biological adhesion

To further find out the molecular mechanism of *Huwe1* in ovarian cancer migration and invasion, we carried out RNAseq to analyze the differences between MOSE-*Huwe1*$^{L/L}$-CreER and MOSE-*Huwe1*$^{L/L}$-Cre cells. Genome-wide analysis identified 25,431 genes, 141 of which had increased expression, and 55 had decreased expression (greater than 2-fold change) (Fig. 4A). Cluster analysis of genes with significant expression differences using the DAVID database showed that the differential genes expressed in the two cells were mainly extracellular matrix-associated genes (Fig. 4B). After reviewing these initial data sets, the gene functions of this set of 648 genes were studied. This included a significant reduction in 22 genes associated with biological adhesion, 10 of which were associated with cell-cell adhesion (Fig. 4C), and upregulation of 12 genes related to biological adhesion (Fig. 4D). Our analysis suggested that some adhesion molecules were up-regulated and some were down-regulated. We suggested that *Huwe1* knockout resulted in increased MOSE cells migration and invasion, owing to the interaction of multiple genes in the extracellular matrix leading to dysregulation of biological connections. The results of the study further confirmed this view.

4. Discussion

Huwe1 catalyzes a range of protein substrates ubiquitination, such as oncogene Myc, the tumor suppressors p53 and BRCA1, DNA damage repair proteins H2AX and the cell cycle protein Cdc6. It suggested that *Huwe1* may be participated in many biological processes regulation, containing tumorigenesis, cell proliferation, migration and

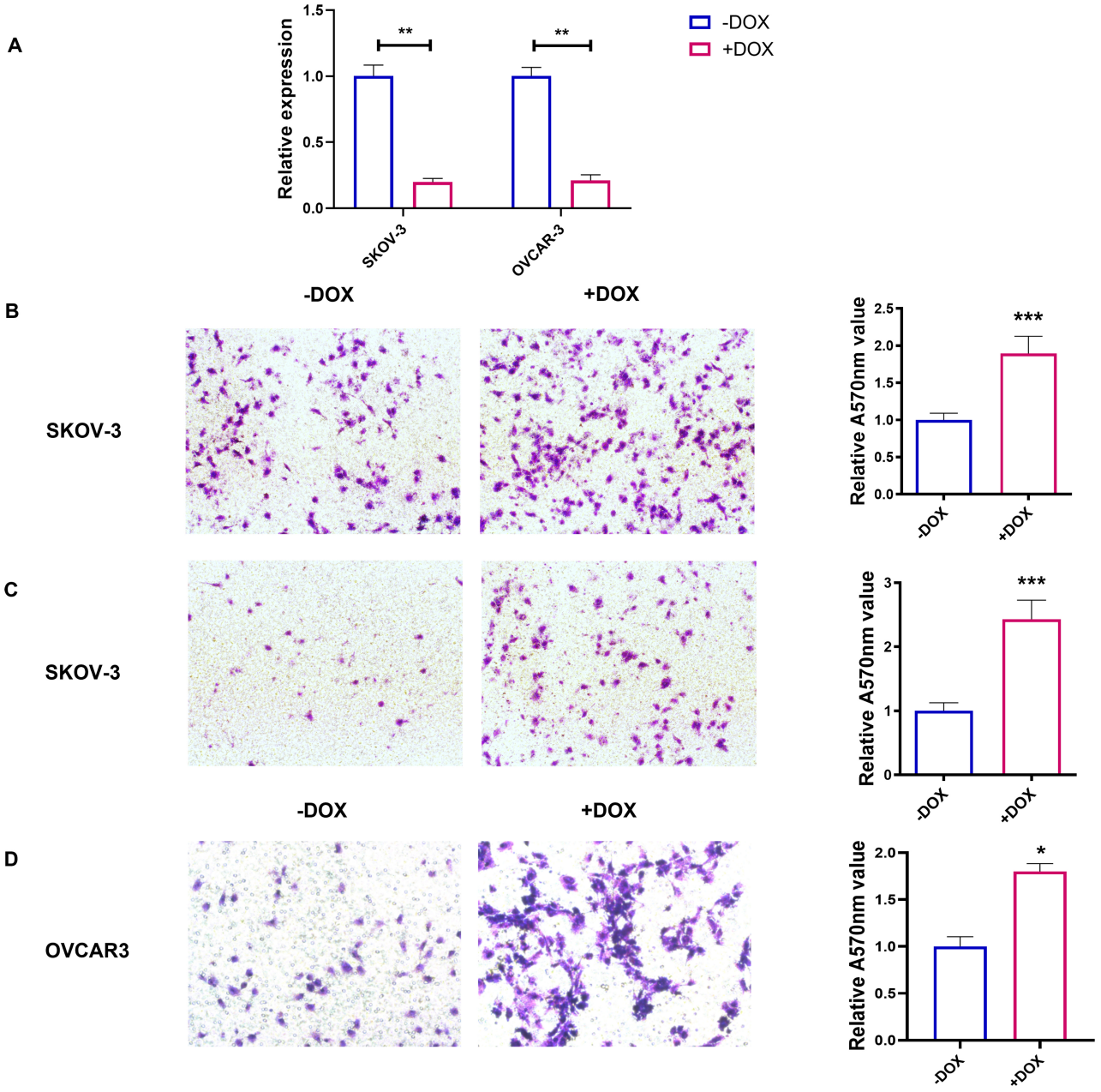

Fig. 3. Silencing *Huwe1* promoted migration and invasion of human ovarian cancer cells. (A) Detection of *Huwe1* inactivation effect in SKOV3 and OVCAR3 cell lines. (B) Analysis of transwell cell migration assay in SKOV3 cells. Scale bar, 100 μm. (C) Analysis of transwell cell invasion assay in SKOV3 cells. Scale bar, 100 μm. (D) Analysis of transwell cell migration assay in OVCAR3 cells. Scale bar, 100 μm. The results are indicated as the mean $\pm$ SD. *, $p < 0.05$, **, $p < 0.01$, ***, $p < 0.001$.

DNA repair [1]. Previous studies reported that *Huwe1* overexpression was associated with cancers of the lung, colon, ovary, and pancreas [1,13]. *Huwe1* promoted the ubiquitination and degradation of the tumor suppressor BRCA1, thereby impeding BRCA1-dependent DNA damage repair in breast cancer cells [14]. Additionally, *Huwe1* promoted gastric cancer cells migration and invasion [15]. However, *Huwe1*, via regulating the stabilization of p53, repressed thyroid cancer progression. *Huwe1* also inhibited the development of mouse skin cancer [16]. *Huwe1* inactivation inhibited the colon cancer cell line proliferation and its tumorigenicity in mice [17]. These results suggested that role of *Huwe1* is diverse in different cancer types.

The existence of metastases and invasion are responsible for most tumor death, but the relationship between *Huwe1* expression and ovarian tumor metastasis has not been reported. In this study, migration was obviously increased in *Huwe1* deletion cells compared with *Huwe1*

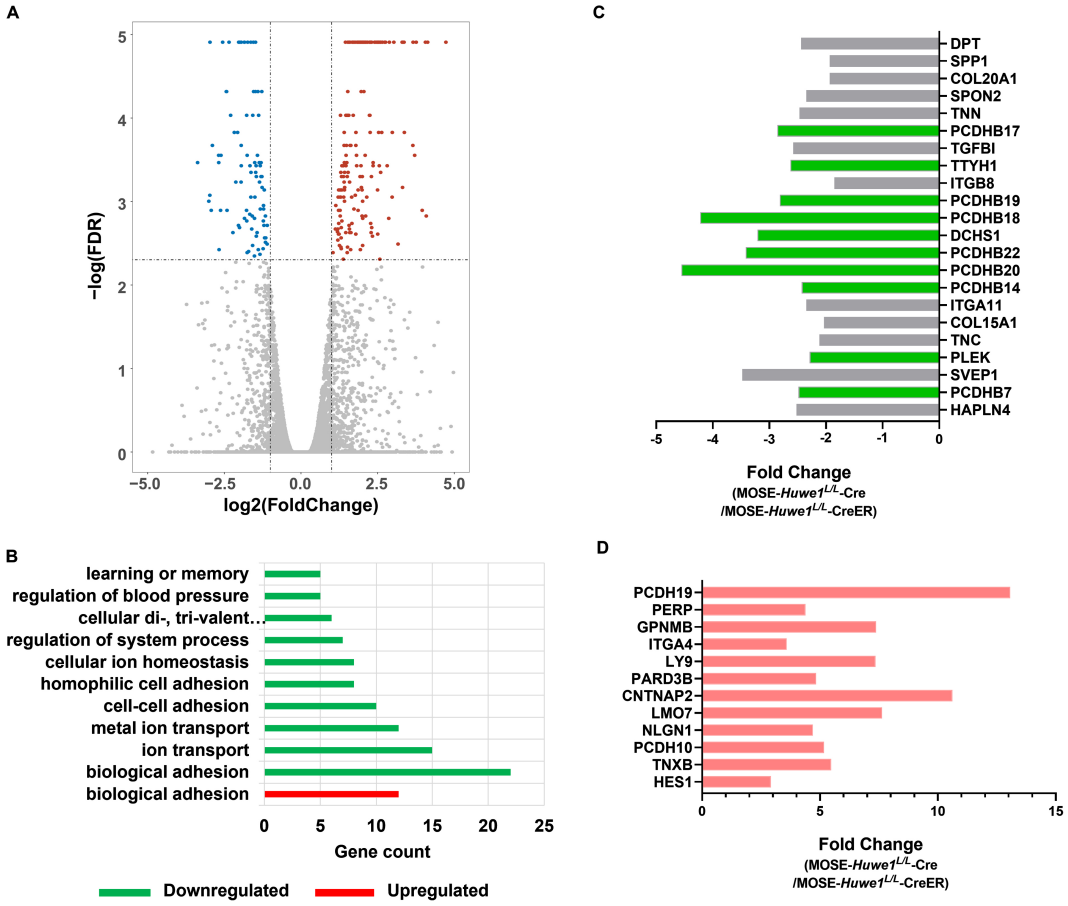

Fig. 4. Enrichment analysis performed for pathways related to cell adhesion after knockout of *Huwe1*. (A) Volcano plot shows significant changes in genes expression (q-value ≤ 0.05 and fold change ≥ 2). (B) Cluster analysis of genes with significant differences in expression using DAVID database, $p < 0.01$. The fold-changes observed in genes that were significantly differentially expressed. There is down-regulation and up-regulation of cell adhesion related genes in MOSE-*Huwe1*$^{L/L}$-Cre cells. (C) Downregulation of bioadhesion-related genes was present in MOSE-*Huwe1*$^{L/L}$-Cre cells, the green represents related down-regulation genes of cell adhesion. (D) Fold change of up-regulation of genes related to biological adhesion, the red represents related up-regulation genes of cell adhesion.

wild-type cells, indicating the knockout of *Huwe1* promoted migration and invasion of MOSE cells. Moreover, the knockout of *Huwe1* caused apparent increase in the number of tumor cells in the blood. Similar to the MOSE cells knockout *Huwe1* experiment, silencing *Huwe1* in human ovarian cancer cell lines showed consistent and significant effects on migration.

ECM, a highly dynamic structure, is composed of collagens, laminins and several other glycoproteins. Not only does the ECMs provided physical scaffolds for cells embedding but also regulated lots of cellular processes, such as growth, differentiation and homeostasis. Some studies even reported that ECM homeostasis deregulation triggered pathological ECM remodeling and even promoted tumor growth and migration [18]. Collagen composition altered obviously in breast cancer where fibrillar collagens I, III and V increased, and type IV collagen was decreased [19]. Heparan sulphate proteoglycans (HSPGs) could be degraded by heparanase (HEP). Under normal physiological conditions, HEP formed heterodimers and did not cleave HSPGs. Nevertheless, under pathological conditions including cancer, HEP drove cleavage of HSPGs promoting cell migration, invasion, and ultimately, metastatic dissemination [20]. Overexpression of the β3 subunit of laminin-332 (LAMB3) promoted colorectal tumor growth and metastasis [21]. Additionally, the ECM-related genes were obviously different in the two cell lines in the study. These results suggested that ECM deregulation influenced many aspects of cancer cell behaviors, such as migration and invasion.

Huwe1, as we know, sustained tumor development via the histone H1.3-H19 cascade. In *Huwe1* deficient cells, increased expression of histone H1.3 could inhibit the expression of non-coding RNA H19 [9]. H19 knockdown led to ten-eleven translocation (TET) family proteins3 (TET3) downregulation through H19/let-7 axis. TET3 downregulation repressed TGF-β signaling and its downstream signaling molecules, such as TGFBR2, TGFBR1 and Smad pro-

teins, ultimately leading to ECM change [22]. To explore the relationship between *Huwe1*, ECM, and tumor migration, and to validate whether *Huwe1* inhibits cell migration by regulating some mechanism of the ECM, we performed RNAseq. Cluster analysis of genes with significant expression differences was performed using the DAVID database. It showed that the genes with differential expression in the two cell lines were mainly ECM-related genes. Loss of *HAPLN4*, *SVEP1*, and *DPT* were positively correlated with migration and invasion of tumor cells in previous studies [23–25]. Our data further confirmed that these genes were significantly downregulated in the MOSE-*Huwe1*$^{L/L}$-*Cre* group. Upregulation of *HES1*, *CNTNAP2*, and *PCDH19* positively correlated with migration and invasion of tumor cells also have been demonstrated [26–29], and these genes were significantly upregulated in the MOSE-*Huwe1*$^{L/L}$-*Cre* group. The results demonstrated that the increase of MOSE cells migration and invasion induced by *Huwe1* knockout might be due to the ECM homeostasis deregulation caused by multiple gene changes.

Apart from changing the ECM to promote metastasis via the histone H1.3-H19 cascade, the regulation of various substrates by *Huwe1* may involve cell invasion and migration [3,4]. For example, the c-Myc/Miz1 complex accumulation, the tumor suppressor p53 loss and other related proteins can promote cell spreading and migration [16,30]. Besides, in a comprehensive bioinformatics analysis of ENO1-related genes, the researchers identified three hub genes including *Huwe1*, all of which are involved in tumor metastasis [31]. However, the specific mechanism of the ECM affecting ovarian cancer cell migration and invasion, remain to the further research.

5. Conclusions

In summary, this study demonstrated that inactivation of *Huwe1* promoted ovarian cancer cells migration and invasion. Moreover, the metastatic inhibitory effect of *Huwe1* in ovarian cancer due to its involvement in the homeostasis regulation of ECM.

Author contributions

DY designed the research study. FZ, JG and SY performed the research. FZ and YM analyzed the data. FZ, JG and XZ wrote the manuscript. All authors contributed to editorial changes in the manuscript. All authors read and approved the final manuscript.

Ethics approval and consent to participate

All animal experiments approved by the animal ethics committee of the Kunming Institute of Zoology, Chinese Academy of Sciences (SMKX-20160922-01).

Acknowledgment

We would like to thank all the peer reviewers for their valuable comments and suggestions, which helped to greatly improve the quality of our manuscript.

Funding

This work was supported by the [Science and Technology Department of Sichuan Province #1] under Grant [2020JDRC0019]; [Science and Technology Department of Yunnan Province #2] under Grant [2019FB115], and [1.3.5 project for disciplines of excellence; West China Hospital, Sichuan University #3] under Grant [ZYYC20002].

Conflict of interest

The authors declare no conflict of interest.

Supplementary material

Supplementary material associated with this article can be found, in the online version, at https://www.imrpress.com/journal/EJGO/43/1/10.31083/j.ejgo4301013.

References

[1] Yang D, Cheng D, Tu Q, Yang H, Sun B, Yan L, *et al*. *Huwe1* controls the development of non-small cell lung cancer through down-regulation of p53. Theranostics. 2018; 8: 3517–3529.

[2] Su C, Wang T, Zhao J, Cheng J, Hou J. Meta-analysis of gene expression alterations and clinical significance of the HECT domain-containing ubiquitin ligase *Huwe1* in cancer. Oncology Letters. 2019; 18: 2292–2303.

[3] Vaughan L, Tan C, Chapman A, Nonaka D, Mack NA, Smith D, *et al*. *Huwe1* Ubiquitylates and Degrades the RAC Activator TIAM1 Promoting Cell-Cell Adhesion Disassembly, Migration, and Invasion. Cell Reports. 2015; 10: 88–102.

[4] Ma W, Zhao P, Zang L, Zhang K, Liao H, Hu Z. Tumour suppressive function of *Huwe1* in thyroid cancer. Journal of Biosciences. 2016; 41: 395–405.

[5] Yeung T, Leung CS, Yip K, Au Yeung CL, Wong STC, Mok SC. Cellular and molecular processes in ovarian cancer metastasis. a Review in the Theme: Cell and Molecular Processes in Cancer Metastasis. American Journal of Physiology-Cell Physiology. 2015; 309: C444–C456.

[6] Lowry KP, Lee SI. Imaging and Screening of Ovarian Cancer. Radiologic Clinics of North America. 2017; 55: 1251–1259.

[7] Su C, Wang T, Zhao JB, Cheng J, Hou JJ. Meta-analysis of gene expression alterations and clinical significance of the HECT domain-containing ubiquitin ligase *Huwe1* in cancer. Oncology Letters. 2019; 18: 2292–2303.

[8] Podgorska A, Rembiszewska A, Szafron L, Konopka B, Lukasik M, Budzilowska A, *et al*. Clinical significance of *Huwe1* expression in ovarian cancer. European Journal of Cancer. 2015; 51: S94.

[9] Yang D, Sun B, Zhang X, Cheng D, Yu X, Yan L, *et al*. *Huwe1* Sustains Normal Ovarian Epithelial Cell Transformation and Tumor Growth through the Histone H1.3-H19 Cascade. Cancer Research. 2017; 77: 4773–4784.

[10] Flesken-Nikitin A, Hwang CI, Cheng CY, Michurina TV, Enikolopov G, Nikitin AY. Ovarian surface epithelium at the junction area contains a cancer-prone stem cell niche. Nature. 2013; 495: 241–245.

[11] Friedmann-Morvinski D, Bushong EA, Ke E, Soda Y, Marumoto

T, Singer O, *et al*. Dedifferentiation of neurons and astrocytes by oncogenes can induce gliomas in mice. Science. 2012; 338: 1080–1084.

[12] Trapnell C, Roberts A, Goff L, Pertea G, Kim D, Kelley DR, *et al*. Differential gene and transcript expression analysis of RNA-seq experiments with TopHat and Cufflinks. Nature Protocols. 2012; 7: 562–578.

[13] Confalonieri S, Quarto M, Goisis G, Nuciforo P, Donzelli M, Jodice G, *et al*. Alterations of ubiquitin ligases in human cancer and their association with the natural history of the tumor. Oncogene. 2009; 28: 2959–2968.

[14] Wang X, Lu G, Li L, Yi J, Yan K, Wang Y, *et al*. *Huwe1* interacts with BRCA1 and promotes its degradation in the ubiquitin-proteasome pathway. Biochemical and Biophysical Research Communications. 2014; 444: 549–554.

[15] He Y, Zhou J, Wan Q. The E3 ligase *Huwe1* mediates TGFBR2 ubiquitination and promotes gastric cancer cell proliferation, migration, and invasion. Investigational New Drugs. 2021; 39: 713–723.

[16] Inoue S, Hao Z, Elia AJ, Cescon D, Zhou L, Silvester J, *et al*. Mule/*Huwe1*/Arf-BP1 suppresses Ras-driven tumorigenesis by preventing c-Myc/Miz1-mediated down-regulation of p21 and p15. Genes and Development. 2013; 27: 1101–1114.

[17] Peter S, Bultinck J, Myant K, Jaenicke LA, Walz S, Müller J, *et al*. Tumor cell-specific inhibition of MYC function using small molecule inhibitors of the *Huwe1* ubiquitin ligase. EMBO Molecular Medicine. 2014; 6: 1525–1541.

[18] Yuzhalin AE, Gordon-Weeks AN, Tognoli ML, Jones K, Markelc B, Konietzny R, *et al*. Colorectal cancer liver metastatic growth depends on PAD4-driven citrullination of the extracellular matrix. Nature Communications. 2018; 9: 4783.

[19] Oskarsson T. Extracellular matrix components in breast cancer progression and metastasis. Breast. 2013; 22: S66–S72.

[20] Barash U, Cohen-Kaplan V, Dowek I, Sanderson RD, Ilan N, Vlodavsky I. Proteoglycans in health and disease: new concepts for heparanase function in tumor progression and metastasis. The FEBS Journal. 2010; 277: 3890–3903.

[21] Zhu Z, Song J, Guo Y, Huang Z, Chen X, Dang X, *et al*. LAMB3 promotes tumour progression through the AKT–FOXO34 axis and is transcriptionally regulated by the BRD2/acetylated ELK4 complex in colorectal cancer. Oncogene. 2020; 39: 4666–4680.

[22] Cao T, Jiang Y, Wang Z, Zhang N, Al-Hendy A, Mamillapalli R, *et al*. H19 lncRNA identified as a master regulator of genes that drive uterine leiomyomas. Oncogene. 2019; 38: 5356–5366.

[23] Sim H, Hu B, Viapiano MS. Reduced expression of the hyaluronan and proteoglycan link proteins in malignant gliomas. The Journal of Biological Chemistry. 2009; 284: 26547–26556.

[24] Chen L, Liu D, Yi X, Qi L, Tian X, Sun B, *et al*. The novel miR-1269b-regulated protein SVEP1 induces hepatocellular carcinoma proliferation and metastasis likely through the PI3K/Akt pathway. Cell Death and Disease. 2020; 11: 320.

[25] Wang W, Gao W, Zhang L, Zhang D, Zhao Z, Bao Y. Deoxypodophyllotoxin inhibits cell viability and invasion by blocking the PI3K/Akt signaling pathway in human glioblastoma cells. Oncology Reports. 2019; 41: 2453–2463.

[26] Bhatnagar R, Dabholkar J, Saranath D. Genome-wide disease association study in chewing tobacco associated oral cancers. Oral Oncology. 2012; 48: 831–835.

[27] Yao X, Zhang H, Liu Y, Liu X, Wang X, Sun X, *et al*. MiR-99b-3p promotes hepatocellular carcinoma metastasis and proliferation by targeting protocadherin 19. Gene. 2019; 698: 141–149.

[28] Gao F, Huang W, Zhang Y, Tang S, Zheng L, Ma F, *et al.* Hes1 promotes cell proliferation and migration by activating Bmi-1 and PTEN/Akt/GSK3β pathway in human colon cancer. Oncotarget. 2015; 6: 38667–38680.

[29] Li Y, Zhang Y, Liu X, Wang M, Wang P, Yang J, *et al*. Lutein inhibits proliferation, invasion and migration of hypoxic breast cancer cells via downregulation of HES1. International Journal of Oncology. 2018; 52: 2119–2129.

[30] Yi Y, Tsai SH, Cheng JC, Wang EY, Anglesio MS, Cochrane DR, *et al*. APELA promotes tumour growth and cell migration in ovarian cancer in a p53-dependent manner. Gynecologic Oncology. 2017; 147: 663–671.

[31] Huang Z, Lin B, Pan H, Du J, He R, Zhang S, *et al.* Gene expression profile analysis of ENO1 knockdown in gastric cancer cell line MGC-803. Oncology Letters. 2019; 17: 3881–3889.